land

MDPI

*Article*

# Intelligent Recommendation of Multi-Scale Response Strategies for Land Drought Events

**Lei He [1,2], Yuheng Lei [1,2], Yizhuo Yang [3], Bin Liu [1,2], Yuxia Li [3], Youcai Zhao [1] and Dan Tang [1,*]**

[1] School of Software Engineering, Chengdu University of Information Technology, Chengdu 610225, China
[2] Sichuan Province Engineering Technology Research Centre of Support Software of Informatization Application, Chengdu 610225, China
[3] School of Automation, University of Electronic Science and Technology of China, Chengdu 611731, China
* Correspondence: tangdan@cuit.edu.cn

**Abstract:** Currently, land drought events have become a frequent and serious global disaster. How to address these droughts has become a major issue for researchers. Traditional response strategies for land drought events have been determined by experts based on the severity levels of the events. However, these methods do not account for temporal variations or the specific risks of different areas. As a result, they overlooked the importance of spatio-temporal multi-scale strategies. This research proposes a multi-scale response strategy recommendation model for land drought events. The model integrates characteristics of drought-causing factors, disaster-prone environments, and hazard-bearing bodies using case-based reasoning (CBR). Additionally, the analytic hierarchy process (AHP) and entropy weighting methods (EWMs) are introduced to assign weights to the feature attributes. A case retrieval algorithm is developed based on the similarity of these attributes and the structural similarities of drought cases. The research further classifies emergency strategies into long-term and short-term approaches. Each approach has a corresponding correction algorithm. For short-term strategies, a correction algorithm based on differential evolutions is applied. For long-term strategies, a correction algorithm based on drought risk assessment is developed. The algorithm considers factors such as drought risk, vulnerability, and exposure. It facilitates multi-scale decision-making for drought events. The candidate case obtained using the correction algorithm shows an overall attribute similarity of 94.7% with the real case. The emergency response levels match between the two cases. However, the funding required in the candidate case is CNY 327 million less than the actual expenditure.

**Keywords:** land; drought events; response strategies; risk assessment



Academic Editor: Hanoch Lavee

Received: 6 December 2024
Revised: 20 December 2024
Accepted: 26 December 2024
Published: 28 December 2024

**Citation:** He, L.; Lei, Y.; Yang, Y.; Liu, B.; Li, Y.; Zhao, Y.; Tang, D. Intelligent Recommendation of Multi-Scale Response Strategies for Land Drought Events. *Land* **2025**, *14*, 42. https://doi.org/10.3390/land14010042



## 1. Introduction

Land drought events have gained increasing attention due to their impact on food security and environmental ecology. Research typically focuses on regional factors such as planning, monitoring, early warning, emergency management, and disaster recovery.

In drought planning, Zaniolo et al. [1] developed the multi-scale drought-resistant infrastructure planning model (DRIPP) to optimize dynamic programming strategies for long-term infrastructure deployment and short-term drought response. Frederick A. Armah [2] applied a Markov chain and fuzzy modeling in Ghana to explore the effects of drought and climate change on agriculture and propose strategies for food security. Liu Z emphasized the importance of rainwater management in semi-arid areas with uneven precipitation [3], while Li H developed drought-related environmental policies for the

Lancang River basin [4]. Getirana et al. [5] discuss Brazil's ongoing water crisis, aggravated by frequent droughts and inefficient water management practices. The authors emphasize the urgent need for a comprehensive national drought management plan to address both long-term water resource planning and short-term response strategies.

To manage and reduce the impacts of drought, it is important to create accurate monitoring systems and strong risk assessment plans. Drought monitoring uses different indices and data sources to improve prediction accuracy, while risk assessment looks at possible impacts and helps guide response actions.

In drought monitoring, various indices and multi-source data are used to improve accuracy. Nugraha ASA et al. [6] applied multi-scale imagery and principal component analysis to enhance the temperature vegetation dryness index (TVDI). Li Jing et al. [7] combined MODIS remote sensing data with radial basis function neural networks (RBFNNs) to accurately estimate soil moisture content. Patel N R [8] suggested using NOAA daily rainfall data and the Vegetation Condition Index (VCI) to monitor drought and crop losses in Bundelkhand, accounting for variations in vegetation and geography. Şen Z [9] developed the FSPI method, which fuzzifies the Standardized Precipitation Index (SPI) to improve early warning systems through fuzzy rule sets. Thomaz F R [10] created the Water Scarcity Risk Index (W-ScaRI), which includes sub-indices to assess water scarcity and its impact. In post-disaster recovery, Hoover D L [11] studied grassland vegetation recovery under extreme drought conditions. Yuchi Wang [12] found that a drought monitoring index based on the random forest model achieved high accuracy in drought detection. Junwei Zhou [13] designed the Comprehensive Drought Monitoring Index using an attention-weighted long short-term memory network, which performs better than other models in meteorological and agricultural drought monitoring.

In drought risk assessment and response, Dabanli I [14] used hydrometeorological and economic data from Turkey to evaluate drought hazard, vulnerability, and risk and developed a comprehensive risk map for response strategies. Stolte T R et al. [15] created a multi-dimensional drought risk framework by combining the Water Stress Index (WSI), environmental flow requirements (EFRs), and socio-economic data to predict urban drought risks under future climate scenarios. E Gidey et al. [16] applied the multivariate logit model (MNL) to analyze Ethiopian farmers' response strategies, focusing on how education level and family size affect decision-making. M Wens et al. [17] used social hydrology and agent-based models (ABMs) to study how human behavior impacts drought risk, showing that adaptive decisions can enhance risk assessments. T Tadesse et al. [18] proposed the Drought Resilient and Prepared Africa (DRAPA) framework, integrating social hydrology and ABMs to simulate the effects of adaptive decisions on drought exposure. LA Melsen [19] applied the Variable Infiltration Capacity (VIC) model to simulate floods and droughts in the Tour River basin and examined how subjective modeling choices influence the results.

China is highly susceptible to drought, with frequent and increasingly severe events. Over recent decades, the frequency and intensity of these droughts have risen, largely due to climate change and rapid socio-economic development. According to the China National Climate Center, droughts have impacted over 60% of China's provinces, resulting in significant agricultural losses and posing a threat to water security. Yunnan Province, located in the southwest of China, is particularly vulnerable to these challenges. Its complex terrain, uneven precipitation distribution, and heavy dependence on agriculture make it highly susceptible to drought. Over the past 20 years, Yunnan has faced recurrent droughts, with one of the most severe occurring in 2010, affecting over 21 million people and causing direct economic losses of approximately CNY 23.7 billion.

The unique background and drought impact in Yunnan highlight the need for drought response strategies that consider both the specific conditions of the region and the growing

severity of drought events. To address these challenges, this study proposes an intelligent recommendation model for land drought event response strategies based on case-based reasoning. The model overcomes the limitations of previous research, which relied on single, generic decision-making strategies, failing to account for the spatial and temporal scales of droughts or the specific characteristics of regions like Yunnan.

The model aims to accomplish the following:

(a) Integrate spatial and temporal scales to provide more accurate and dynamic response strategies, overcoming the limitations of single-scale decision-making.
(b) Identify high-risk areas through a comprehensive drought risk assessment model, enabling spatial multi-scale decision-making tailored to the needs of Yunnan.
(c) Bridge short-term crisis management with long-term drought resilience by categorizing strategies into emergency and long-term approaches, ensuring the region can adapt to both immediate and future challenges.

Additionally, the model also combines both quantifiable and non-quantifiable factors, using predictive models to assess the measurable aspects and linking non-quantifiable elements to a response strategy database. It will also provide context-specific recommendations to enhance the understanding and application of drought response strategies.

Through these methods, the model offers more adaptable and detailed responses, providing a tool to address the drought challenges faced by Yunnan Province.

## 2. Data and Methods

### *2.1. Overview of the Research Area*

1. Nature Overview

Yunnan Province, located in southwestern China (Figure 1), has diverse topography, including mountains, basins, and plains. Research [20,21] shows that these features contribute to varying micro-climates and significant drought risks. The land use is predominantly forested (63%), with cultivated land covering 13.7%. Much of this cultivated land is used for dryland farming, making the region highly susceptible to drought. The province experiences small annual temperature fluctuations but large daily variations, with distinct wet and dry seasons. Precipitation levels vary considerably across the region. For example, Nujiang receives over 1800 mm annually, whereas Yuxi receives less than 632 mm. These geographical and climatic factors play a crucial role in influencing water availability and drought occurrence in the region.

2. Social Overview

Yunnan Province has eight prefecture-level cities, eight autonomous prefectures, 17 municipal districts, 18 county-level cities, 65 counties, and 29 autonomous counties. The total population is 45.956 million, with 15.337 million ethnic minorities, making up 33.37% of the total. This represents a 7.3% increase from the previous year. According to the third national land survey, Yunnan had 5.3783 million hectares of cultivated land, 1.3178 million hectares of grassland, and 24.9449 million hectares of woodland. Additionally, the province had 24.969 million hectares of forest land. Cultivated land was primarily in Pu'er and four other prefectures, grassland was mainly in Dongchuan and two other counties, and woodland was concentrated in Luquan and two other counties.

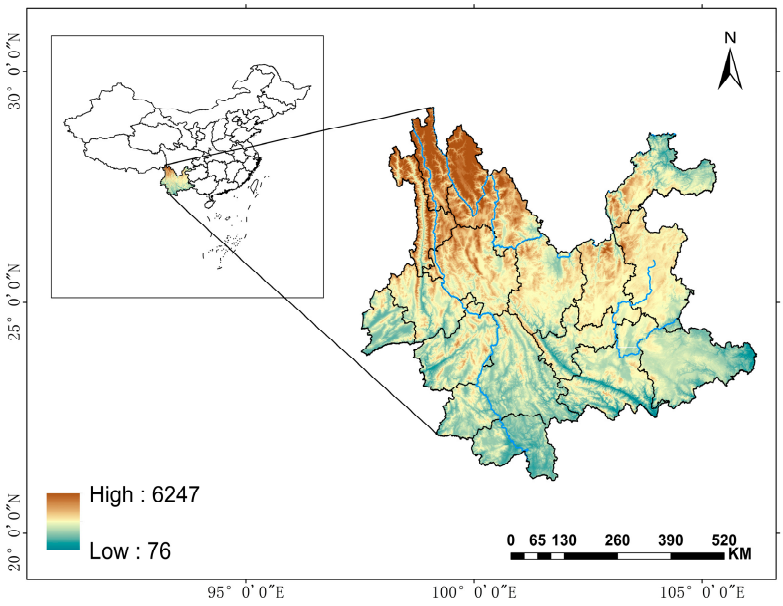


**Figure 1.** Geographical location of Yunnan Province.

### *2.2. Overview of the Target Case*

In spring 2019, Yunnan Province faced a severe drought, with precipitation from January to June 32% below average. Notably, from 1 to 20 May, rainfall was just 6.6 mm, an 88.6% reduction. During this period, temperatures exceeded 35 °C on 335 occasions. By June, widespread soil moisture shortages persisted, affecting 1090.67 thousand hectares of crops. Additionally, 2.16 million people faced drinking water shortages. The changes in key indicators during the dry period in Yunnan Province in 2019 are shown in Figure 2.

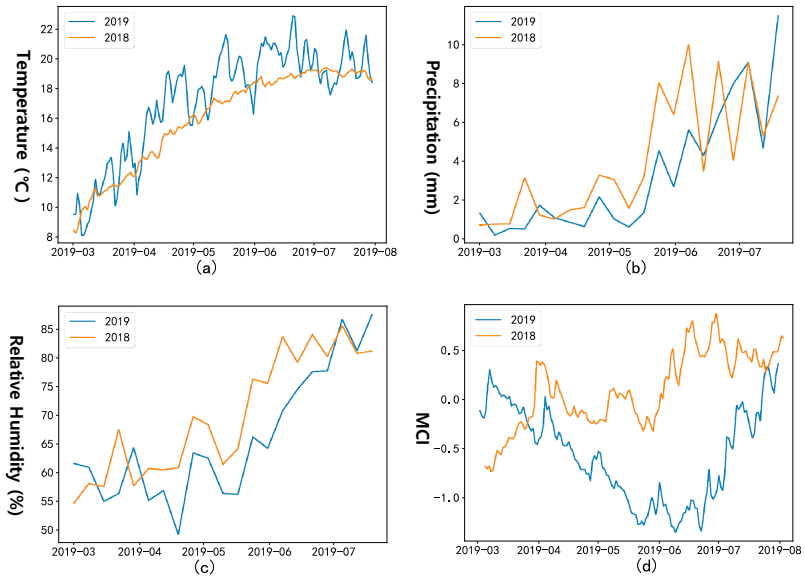


**Figure 2.** Comparison of main indicators during the dry period in Yunnan Province in 2019. ((**a**) Temperature; (**b**) precipitation; (**c**) relative humidity; (**d**) MCI).

Post-drought, Yunnan Province issued red alerts for meteorological drought, with sustained high forest fire risks. On 21 May, a Level IV emergency response was initiated, with CNY 570 million allocated for relief efforts.

### 2.3. Data

- Historical case data

The north and southwest regions of China are frequently affected by severe droughts, making them key areas for drought research. Previous data had gaps, but the data from 2015 to 2019 are more comprehensive and complete. Therefore, this research selects drought-related data from this period, covering ten provinces and cities in these regions. The data, sourced from the China Disaster Reduction Network and the China Flood and Drought Bulletin, include information on the timing, location, emergency response levels, and relief fund investments.

- Meteorological data

Meteorological data, including precipitation, temperature, relative humidity, and wind speed, are selected from the CN05.1 grid observation dataset, which has a spatial resolution of 0.25° [22–24]. The comprehensive drought index and standard precipitation index data are obtained from the National Climate Center.

- Socioeconomic data

This chapter examines socio-economic data, including GDP, population, and the proportion of agricultural GDP, to assess a region's resilience to drought. A higher GDP generally reflects better resources for drought mitigation, while population data help evaluate the potential human impacts and vulnerability. Regions with a larger proportion of agricultural GDP are more dependent on climate conditions and thus more vulnerable to drought. GDP and population data were obtained from the China GDP and Population Spatial Distribution Dataset (Institute of Geographic Sciences and Natural Resources Research, Chinese Academy of Sciences) [25]. The proportion of agricultural GDP was sourced from regional statistical yearbooks. Data on cultivated land and pasture areas were sourced from the China Multi-Period Land Use Remote Sensing Monitoring Datasets (CNLUCC) [26]. These land use types, particularly agricultural land, are key indicators of socio-economic vulnerability to drought. By linking land use data with socio-economic indicators, we can better understand how a region's structure influences its drought resilience.

- Response measures data

The drought emergency response data in this section are derived from provincial emergency response plans for flood control and drought relief, issued by the relevant emergency management departments. Long-term drought response strategies were collected from publicly available internet sources.

- SPI and MCI

The SPI [27] is used to measure precipitation anomalies over a period, indicating the severity of drought conditions. It is typically calculated for different time scales (e.g., 1, 3, 6, 12 months) to capture droughts of varying durations. The MCI [28] is a composite drought index that incorporates multiple meteorological variables (e.g., precipitation, temperature) to assess the overall meteorological drought conditions. The MCI is more comprehensive, as it integrates both short-term and long-term drought patterns.

Both the SPI and MCI are essential tools for drought assessment. While the SPI primarily focuses on precipitation and is commonly used in early warning systems, the MCI incorporates additional variables, such as temperature, to identify regions vulnerable to long-term drought effects. The integration of these two indices provides a more comprehensive understanding of drought dynamics, enabling decision-makers to develop more targeted and effective mitigation strategies.

The raster data used in this research are shown in Table 1.

**Table 1.** Raster data situation table.

| Data Name | Units | Timespan | Data Sources | Spatial Resolution |
|---|---|---|---|---|
| precipitation | mm | 2000–2020 | CN05.1 latticed observation dataset | 0.25° |
| temperature | °C | 2000–2020 | CN05.1 latticed observation dataset | 0.25° |
| wind speed | m/s | 2000–2020 | CN05.1 latticed observation dataset | 0.25° |
| relative humidity | % | 2000–2020 | CN05.1 latticed observation dataset | 0.25° |
| MCI | No unit | 2000–2020 | National Climate Center | 0. 5° |
| SPI | No unit | 2000–2020 | National Climate Center | 0. 5° |
| GDP | ¥10,000/km$^2$ | 2000–2020 | China GDP spatial distribution km grid datasets | 1 Km |
| population | people/km$^2$ | 2000–2020 | China GDP spatial distribution km grid datasets | 1 Km |
| land utilization | % | 2000–2020 | Multi-period land use remote sensing monitoring datasets in China | 30 m |

### *2.4. Methods*

The methods employed in this study include run theory for identifying drought events, extraction of drought intensity, case representation, case retrieval, case correction, and case preservation algorithms. The overall methodological framework is illustrated in Figure 3.

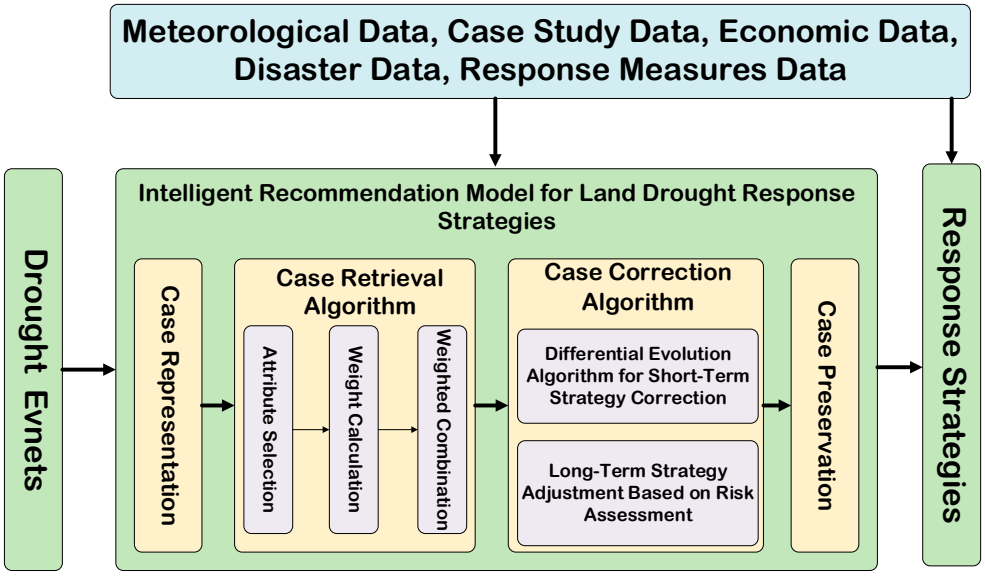


**Figure 3.** Methodological framework.

#### 2.4.1. Drought Event Identification and Intensity Attribute Extraction Using Run Theory

A drought case includes factors such as drought causes, pre-disaster environmental conditions, carrying capacity, and resulting losses. The main content is shown in Table 2.

This section uses run-length theory to analyze the Meteorological Drought Index (MCI) sequence, determining the start and end times of drought more precisely. Additionally, it incorporates the drought severity attribute (DM) extracted from the sequence into the drought case content for a more precise description of the drought.

**Table 2.** Data content and descriptions table.

| Data Type | Specific Content | Description |
|---|---|---|
| Basic Information | Start time (STD), end time (EDT), affected area (Location), drought type (TYPE), etc. | These data are crucial for determining the extent and severity of the drought and helps take timely, location-specific response actions. |
| Meteorological Information | Precipitation (PRE), temperature (TMP), wind speed (WIN), relative humidity (RHU), etc. | These variables help identify the meteorological conditions contributing to the drought, track its development, and evaluate its intensity and duration. |
| Drought Index Information | Standardized Precipitation Index (SPI), Meteorological Drought Index (MCI), etc. | These indices quantify drought severity and enable standardized comparisons across regions and periods for better monitoring and decision-making. |
| Socio-economic Information | Gross domestic product (GDP), population data (POP), land use data, water supply and demand data, etc. | These factors reflect how well a region can withstand and recover from drought and identify the most affected socio-economic groups. |
| Drought Disaster Data | Direct economic losses, affected crop area, number of affected people, etc. | These data are vital for assessing drought damage and for planning recovery strategies. |
| Response Strategy Data | Drought response level (Level), financial investment (Cost), and other measures to reduce drought risk. | These data help evaluate the effectiveness of drought management strategies and guide future responses to mitigate impacts. |

Figure 4 illustrates a scenario for daily MCI data $Z_t$ across a specific time interval. Drought occurrence is evaluated using national meteorological drought level standards. A threshold Z is established according to the criteria in Table 3, with mild drought defined as Z = −0.5 in this research. Positive and negative runs represent continuous sequences above and below the threshold, indicating periods of no drought and drought, respectively. The length of negative runs indicates drought duration (D), with the start and end points marking drought onset and termination. The cumulative MCI value during negative runs signifies drought severity (M). Temporary rainfall within the drought period can produce shorter "sub-droughts", such as $d_1$ and $d_3$. The severities of these sub-droughts ($m_1$ and $m_2$) are recorded, though they remain part of the same drought event. Therefore, when short-term rainfall occurs during a drought, it will not be mistakenly classified as a separate drought event. This improves the accuracy of drought identification. Incorporating sub-drought events allows for capturing variations in drought conditions, providing a more detailed representation of drought dynamics, particularly in regions with fluctuating conditions. Thus, the start time of $d_1$ is taken as the onset of the current drought and the end time of $d_3$ as the termination. The combined severity of $m_1$ and $m_2$ represents the overall drought intensity.

Across 20 drought identification tests, the run-length theory-based method accurately identified drought onset and termination in 19 cases, achieving an accuracy rate of 95%.

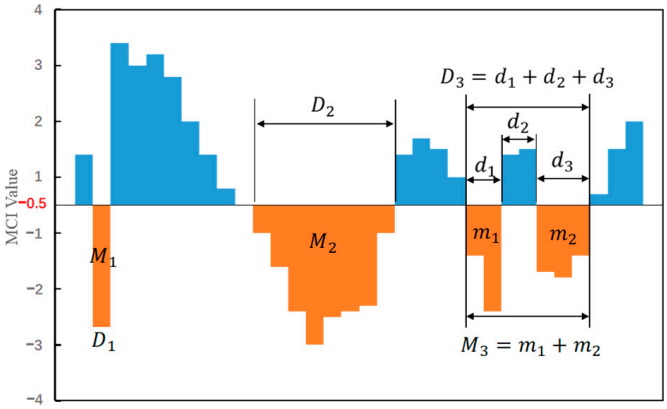


**Figure 4.** Determination of drought case start and end times ($D$) and drought severity ($M$) using MCI data and run-length theory.

**Table 3.** Classification table of meteorological drought composite index levels [29].

| Level | Type | MCI |
|---|---|---|
| 1 | no drought | $-0.5 \leq$ MCI |
| 2 | mild drought | $-1.0 \leq$ MC $\leq -0.5$ |
| 3 | moderate drought | $-1.5 \leq$ MC $\leq -1.0$ |
| 4 | severe drought | $-2.0 \leq$ MC $\leq -1.5$ |
| 5 | extreme drought | MC $\leq -2.0$ |

#### 2.4.2. Algorithm for Case Retrieval in Drought Events

1. Feature attribute selection and attribute similarity calculation

Drought case feature attributes include basic information (time, location, and drought type), meteorological data (precipitation, temperature, humidity, and wind speed), drought indices (SPI and MCI), and socio-economic factors (GDP and population). These attributes are crucial for understanding the characteristics of droughts and for assessing the appropriate response strategies. Time and location variations play a significant role, and socio-economic factors such as GDP and population help evaluate a region's vulnerability and resilience.

For similarity calculation, numerical attributes are calculated using the formula from Zhang Mingming's research [30].

$$\mathrm{Y}_i = \sqrt{\max\left\{(max_i - x_i)^2, (min_i - x_i)^2\right\}} \tag{1}$$

$$Sim(X_i, Y_i) = \exp\left(-\frac{\sqrt{(x_i - y_i)^2}}{\mathrm{Y}_i}\right) \tag{2}$$

For enumerated data, such as drought type, similarity is calculated using the following formula:

$$Sim(X_i, Y_i) = \begin{cases} 0 \; x_i \neq y_i \\ 1 \; x_i \neq y_i \end{cases} \tag{3}$$

where $x_i$ and $y_i$ are the values of the ith feature attribute of the target case $X$ and historical case $Y$, respectively. $max_i$ and $min_i$ are the upper and lower limits of the value of the $ith$ feature attribute, respectively. $Sim(X_i, Y_i)$ represents the similarity of the ith feature attribute between the target case $X$ and the historical case $Y$. $Sim(X_i, Y_i) \in [0, 1]$.

2. Calculating the subjective and objective weights of drought events

The analytic hierarchy process (AHP) is used to determine the relative importance of each feature attribute and establish a hierarchical model. The first level includes basic information, meteorological data, and socio-economic data, while the second level contains sub-items from these categories. The hierarchy is shown in Figure 5.

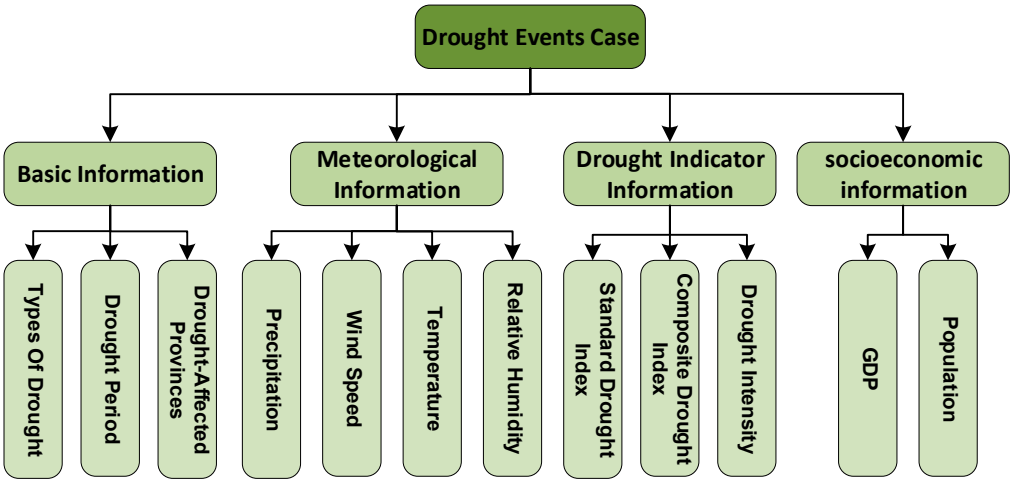


**Figure 5.** Drought event case hierarchy.

For each level, a judgment matrix is constructed. Domain experts compare the elements in the matrix pairwise to determine their relative importance or priority. Assuming there are $n$ feature attributes at a given level, where $i$ and $j$ represent the $i\_th$ and $j\_th$ attributes, the resulting judgment matrix $W$ is shown in Equation (4).

$$W = \begin{bmatrix} w_{11} & \cdots & w_{1n} \\ \vdots & \ddots & \vdots \\ w_{n1} & \cdots & w_{nn} \end{bmatrix} \tag{4}$$

Based on the judgment matrix $W$, the maximum eigenvalue $\alpha_{max}$ and the corresponding maximum eigenvector $\omega$ are calculated. Their relationship is shown in Equation (5).

$$q \times \omega_1 = \alpha_{max} \times \omega_1 \tag{5}$$

The value of the maximum eigenvector represents the weight of the corresponding indicator.

After calculating the feature attribute weights, consistency should be checked. This ensures the results are reliable. The consistency index ($CI$) and consistency ratio ($CR$) are calculated as follows:

$$CI = \frac{\alpha_{max} - n}{n - 1} \tag{6}$$

$$CR = \frac{CI}{RI} \tag{7}$$

Here, $n$ represents the number of feature attributes and $CR$ is the consistency index used to access the reasonableness of the discriminant matrix. A $CR$ value less than 0.1 indicates satisfactory consistency.

Then, the entropy weight method (EWM) is used to calculate the objective weight. The formula for the entropy weight method is as follows:

$$\begin{gathered} Q_{ij} = \frac{Sim^j(c_0, c_i)}{\sum_{z=1}^{m} Sim^j(c_0, c_z)} \\ E_j = -\left(lna_j\right)^{-1} \sum_{i=1}^{m} Q_{ij} ln Q_{ij} \\ \omega_2 = \frac{1 - E_j}{n - \sum_{j=1}^{n} E_j} \end{gathered} \tag{8}$$

where $\omega_2$ is the objective weight value determined by the entropy weight method and $Sim^j(c_0, c_i)$ represents the similarity between the feature attributes of current drought cases and historical cases. $n$ is the number of feature attributes, $m$ is the number of historical cases, and $a_j$ represents the number of non-null values of feature attribute $j$.

Finally, the weights are integrated. The subjective and objective weights are integrated by linear weighting [31]. Let $\omega_1$ be the subjective weight vector, $\omega_2$ be the objective weight vector, and $\omega$ be the combination weight obtained by linear weighting. The combination method is described in Equation (9).

$$\begin{gathered} \omega = \alpha\omega_1 + (1 - \alpha)\omega_2 \\ \alpha = \frac{n}{n-1}\left[\frac{2}{n}(p_1 + p_2 + \ldots + np_n) - \frac{n+1}{n}\right] \end{gathered} \tag{9}$$

where $p_i (i = 1, 2, \ldots, n)$ is the vector value of subjective weights sorted in ascending order and n represents the number of feature attributes.

## 3. Global similarity calculation of drought cases

The global similarity between drought cases is calculated using the weighted nearest neighbor algorithm, as shown in Equation (10).

$$Sim(X, Y) = \sum_{i=1}^{n} Sim(X_i, Y_i) \times \omega_i \tag{10}$$

To avoid situations where not all attribute values can be collected at the onset of a drought event, leading to some attributes being assigned a value of 0, which could introduce errors in directly calculating the similarity between two cases, this study incorporates the structural similarity between cases. This approach results in a global similarity calculation formula for drought event cases, as shown in Equation (11).

$$Sim(X, Y) = d_{str} \times \sum_{i=1}^{n} Sim(X_i, Y_i) \times \omega_i \tag{11}$$

$d_{str}$ represents the structural similarity between case $X$ and case $Y$, $Sim(X_i, Y_i)$ represents the similarity between case $X$ and the ith feature attribute of case $Y$, and $\omega_i$ represents the combination weight value of the ith feature attribute. The formula for $d_{str}$ is given in Equation (12).

$$d_{str} = \frac{\omega_{A \cap B}}{\omega_{A \cup B}} \tag{12}$$

A represents the set of non-empty feature attributes of case $X$, $B$ represents the set of non-empty feature attributes of case $Y$, $\omega_{A \cap B}$ represents the weighted sum of all features in the intersection of $A$ and $B$, and $\omega_{A \cup B}$ represents the weighted sum of all features in the union of $A$ and $B$.

The global similarity of all cases is ranked and the case with the highest similarity is output.

2.4.3. Drought Event Case Correction Algorithm

The DE algorithm is employed to retrieve the most similar cases, which serve as the initial population. This is because it can efficiently optimize complex non-linear problems and effectively search large high-dimensional case databases to retrieve the most relevant drought cases. Through operations like mutation, crossover, and selection, candidate cases closest to the current case are generated. The response level and investment of these candidate cases contribute to the target case's drought response emergency strategy.

Initially, the population is established with N similar cases obtained from case retrieval. This population includes two partial feature attribute sets, P and the solution set, S. The feature property table is shown in Table 4.

**Table 4.** Feature property table.

| $p_i$ | DD | MCI | PRE | TMP | WIN | RHU | POP | GDP |
|---|---|---|---|---|---|---|---|---|
| $s_i$ | cost input | Corresponding grade | | | | | | |

Subsequently, the initial fitness function is calculated. As shown in Equation (13), the similarity function of feature attributes between cases is used as the fitness function to calculate the fitness between the historical case $p$ and the current case $p_{new}$.

The fitness function is calculated based on the similarity between the historical case $p$ and the current case $p_{new}$.

$$Fitness(p_i, p_{new}) = \sum_{j=1}^{k} sim(p_{ij}, p_{newj}) \tag{13}$$

The DE algorithm mutates and crosses the population, generating two new populations. A hybrid search mutation operator, combining the best population with random search, balances convergence and diversity. The mutation formula is

$$v_i = x_i + F{\cdot}(x_{best} - x_i) + F{\cdot}(x_{r_1} - x_{r_2}) \tag{14}$$

$x$ denotes the individuals in the population, $0 < I \leq N$; $r_1$ and $r_2$ are positive integers, $0 \leq r_1, r_2, r_3, r_4, r_5 \leq N$, $r_1 \neq r_2 \neq r_3 \neq r_4 \neq r_5 \neq i$; $x_{best}$ is the best individual in the population; and $F$ is the variation scaling factor, usually taking a value between [0,1].

The adaptability of the new population is evaluated by calculating the similarity with the target cases. The selection strategy is applied to choose the best population, as shown by the following formulas:

$$\begin{aligned} p_i &= \begin{cases} p_i' \; if \; Sim(p_i', p_{new}) > Sim(p_i, p_{new}) \\ p_i \; otherwise \end{cases} \\ s_i &= \begin{cases} s_i' \; if \; Sim(p_i', p_{new}) > Sim(p_i, p_{new}) \\ s_i \; otherwise \end{cases} \end{aligned} \tag{15}$$

When the similarity between the generated and target populations meets the specified conditions, the algorithm terminates, the result $s_i$ is output, and $s_i$ is the modified solution of the target case.

For long-term response strategies, this research employs a case correction algorithm for drought events based on drought risk assessment. The key components of the risk assessment are shown in Table 5.

**Table 5.** Attributes and indicators of risk assessment.

| Attribute | Description |
| --- | --- |
| Hazard | This indicates the severity of the drought. In this research, the MCI was selected as the feature factor for the hazard index concerning the relevant literature [32]. |
| Exposure | To represent the number of disaster-bearing bodies exposed to a drought environment, by referring to the relevant literature [33], this research selected population density, the proportion of cultivated land area, and the proportion of pasture area as the feature factors of the exposure index. |
| Vulnerability | To represent the tendency of disaster-bearing bodies to be affected by drought, this study selected the number of reservoirs, GDP, the proportion of agriculture in GDP, water pressure, and other indicators as the feature factors for vulnerability, based on the research of Ahmadalipour et al. [34]. |

This research adopts a drought risk assessment model based on hazard, vulnerability, and exposure, as shown in Equation (16).

$$R = H \times V \times E \tag{16}$$

where $R$ represents the drought risk, $H$ is the hazard index, $V$ is the vulnerability index, and E is the exposure index. The calculation formula of each index is shown in Equation (17).

$$H = p \times \omega$$

$$E = \sum_{i=1}^{3} p_i \times \omega_i \tag{17}$$

$$V = \sum_{i=1}^{4} p_i \times \omega_i$$

$p_i$ represents the feature factor of the risk assessment index and $\omega_i$ represents the weight of the assessment factor. The weight shows how much each indicator affects the overall risk. It also combines information from different areas. In this research, the fuzzy analytic hierarchy process (FAHP) is used. Experts give fuzzy scores for each indicator, which create fuzzy intervals to form a fuzzy decision matrix. The fuzzy numbers are then normalized, and the normalized fuzzy features are calculated. The weight of each indicator is found using the geometric mean method. Table 6 shows the normalized factors and weight values for the risk assessment.

**Table 6.** Feature attribute selection and weights of drought risk assessment factors.

| Risk Assessment Indicators | Characterization Factor | The Effect of Feature Factors | Weight |
| --- | --- | --- | --- |
| Risk, H | MCI | Positive | 1 |
| Degree of exposure, E | Density of population | Positive | 0.008 |
| | Proportion of cultivated land area | Positive | 0.926 |
| | Proportion of pasture area | Positive | 0.066 |
| Vulnerability, V | GDP | Positive | 0.001 |
| | Agriculture as a share of GDP | Positive | 0.876 |
| | Pressure of water | Positive | 0.016 |
| | Number of reservoirs | Positive | 0.107 |

To facilitate the identification of high-risk areas, this research rasterizes the feature factor data and computes the drought risk assessment results of the research area based on raster data. Figure 6 shows the calculation process.

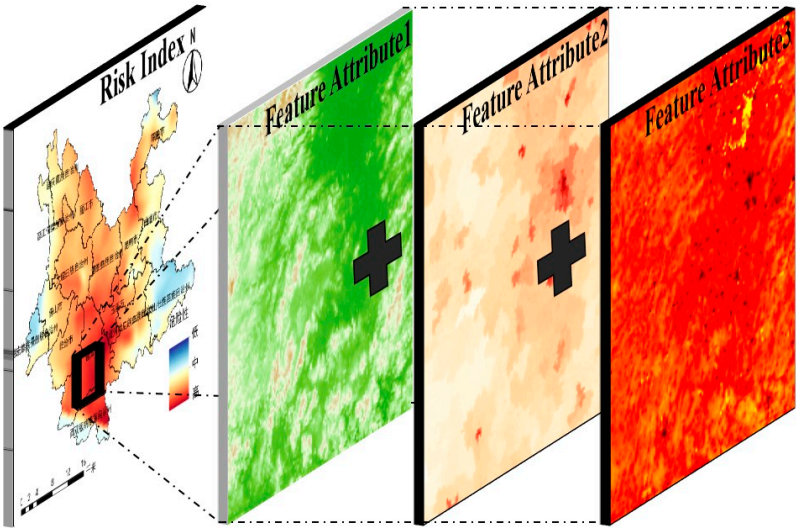


**Figure 6.** Rasterized risk assessment index calculation method.

Then, based on the results from the drought risk assessment, the indicators for hazard, vulnerability, and exposure are classified. From a drought risk reduction perspective, long-term drought response strategies are then specified. These strategies are tailored to different categories of indicators, with corresponding recommendations presented in Table 7.

**Table 7.** Long-term strategies of drought high-risk response under different risk types.

| Types of Risk | Response Strategies | The Strategy $p_i$ That can be Quantified |
|---|---|---|
| High-hazard area | Optimized water resource allocation, widespread rainwater collection, and water-efficient agriculture. | Water resource allocation |
| High-exposure area | Restrict cropland areas, enforce reforestation policies, and enhance cultivated land protection. | Farmland converted to forest and population density |
| High-vulnerability area | Industrial restructuring, non-agricultural economic development promotion, agricultural product processing, and industrial transformation promotion. | Agriculture as a percentage of GDP |

In this research, the purpose of reducing the corresponding risk index value is to achieve the purpose of case correction by improving the quantifiable indicators. The formula for case correction is given in Equation (18).

$$\Delta p_i = \frac{\Delta e}{\omega_i} \tag{18}$$

where $\Delta p_i$ is the correction amount of the quantifiable response strategy, $\Delta e$ is the change quantity of the regional risk index value, and $\omega_i$ is the weight value of the feature factor corresponding to the measure in the calculation of the risk index.

2.4.4. Drought Event Case Preservation Algorithm

In this research, a threshold-based drought case rejection strategy is implemented. (The process is shown in Figure 7). The similarity between new and historical cases is assessed, and a threshold determines whether to include the new case in the historical case base. If the similarity exceeds the threshold (given the limited content in the current historical case database, it is essential to rapidly expand the dataset; therefore, a threshold of 90% has been applied.), indicating redundant knowledge, the new case is discarded. Conversely, if the similarity is below the threshold, indicating valuable new knowledge, the new case is added to the historical case base, thereby enhancing the case-based reasoning (CBR) system's capabilities.

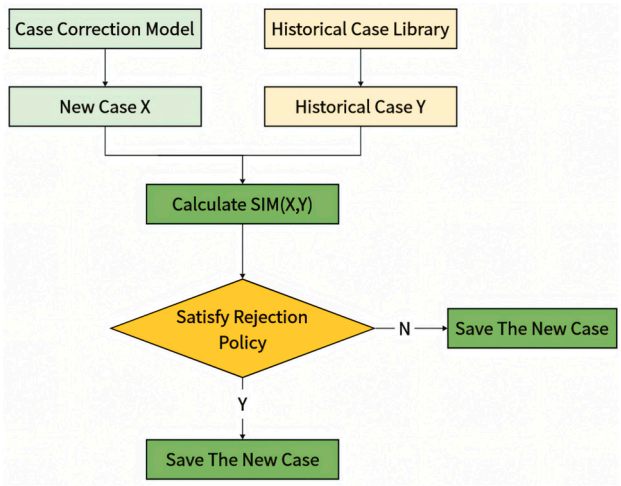


**Figure 7.** Case-saving flowchart.

## 3. Experiment Results and Discussion

In this research, Yunnan Province is taken as the area of study, and the spring drought event of Yunnan Province in 2019 is taken as the target case to analyze the model results and verify the feasibility of the model.

### *3.1. Model Parameter Setting*

In this experiment, the 2019 drought event in Yunnan was used as the target case for the experiment, and the feature attributes are shown in Table 8.

**Table 8.** Feature attribute table of target case (part).

| Location | PRE | WIN | TMP | RHU | DD | GDP | POP | MCI | Level | Cost |
|---|---|---|---|---|---|---|---|---|---|---|
| Yunnan | 4.11 | 2.51 | 19.23 | 68.6 | 11.0 | 2.3 | 48.5 | −1.3 | 4 | 5.7 |

Drought events in North and Southwest China from 2015 to 2019 were selected as the historical cases (excluding the 2019 Yunnan drought). Data samples of drought impacts and decision-making measures from the historical cases are shown in Table 9.

**Table 9.** Historical drought disaster and decision data (Shanxi Province, 2019).

| Financial Loss | Crop-Affected Area | Area of Unharvested Crops | Number of People Affected | Drought Response Level | Invested Capital |
|---|---|---|---|---|---|
| 12.1 | 307.3 | 26.6 | 146.5 | 3 | 20.07 |

This research compiles drought emergency plans from each provincial emergency management department and establishes an emergency response strategy library based on different decision-makers and response levels, as shown in Table 10.

**Table 10.** Emergency response strategy measure database (part).

| Emergency Response Level | Government Sector | Common Population |
|---|---|---|
| IV | Improvement of the utilization efficiency of water resources, such as improving irrigation systems, reducing the loss of water, and so on | Reduce waste of water, such as turning off the tap when brushing your teeth and optimizing water use in your home |
| III | Strengthening water resource management and conservation of restrictions on water use to ensure the safety of the water supply | Cut water waste with fewer car washes, reduced watering, and water-saving shower heads |
| II | Taking emergency measures to ensure the supply of drinking water and domestic water | Minimize water waste with reduced car washing, less watering, and water-saving shower heads |
| I | Emergency water allocation measures to ensure the supply of drinking water and domestic water | Prepare for drought's impact on food, stockpile dry food, and obtain local government's drought warnings and response measures from multiple sources |

### *3.2. Experimental Result*

1. Drought Identification and Case Retrieval Results

In the drought event identification experiment, the run theory-based method successfully identified the start and end times of 19 out of 20 drought events, resulting in a 95% accuracy.

The AHP method is used to score the first level. This generates the judgment matrix $W$. Using Equation (5), the largest eigenvalue of $W$ is $\alpha_{max} = 4.01$, and the largest eigenvector $\omega_1 = [0.21 \quad 0.620.11 \quad 0.06]$. Therefore, the weights for basic information, meteorological data, drought indices, and socio-economic data are 0.21, 0.62, 0.11, and 0.06, respectively. These results are checked using Equations (6) and (7) for consistency. The RI is the random consistency index, with values shown in Table 11.

**Table 11.** RI value table.

| Degree | 2 | 3 | 4 | 5 | 6 | 7 | 8 | 9 |
|---|---|---|---|---|---|---|---|---|
| *RI* | 0 | 0.58 | 0.90 | 1.12 | 1.24 | 1.32 | 1.41 | 1.45 |

CI = 0.0035 is calculated, and the consistency index CR = 0.0038 < 0.1 is calculated by looking up the value of RI through Table 3. Therefore, the evaluation has a satisfactory consistency. The same is true for the second layer. Correlation analysis was conducted on the second-level meteorological data, as shown in Figure 8.

Figure 8 results show that factors such as precipitation, temperature, and humidity are more important than other attributes. This matches the physical processes of drought formation and confirms that the selected feature weights align with actual conditions.

The objective weights are calculated using the EWM. Then, the subjective and objective weights are combined using Equation (9). The combined weights are used to calculate the case similarity. To improve the accuracy of case retrieval, a structural coefficient was introduced. To validate its effectiveness, an experiment was designed to analyze the change in retrieval accuracy before and after its introduction. The case retrieval accuracy is defined as the number of correct cases in the retrieved set, where the correct cases are those

identified by the case retrieval algorithm that matches the target case with complete feature attributes. Figure 9 shows the accuracy of case retrieval after removing different numbers of feature attributes.

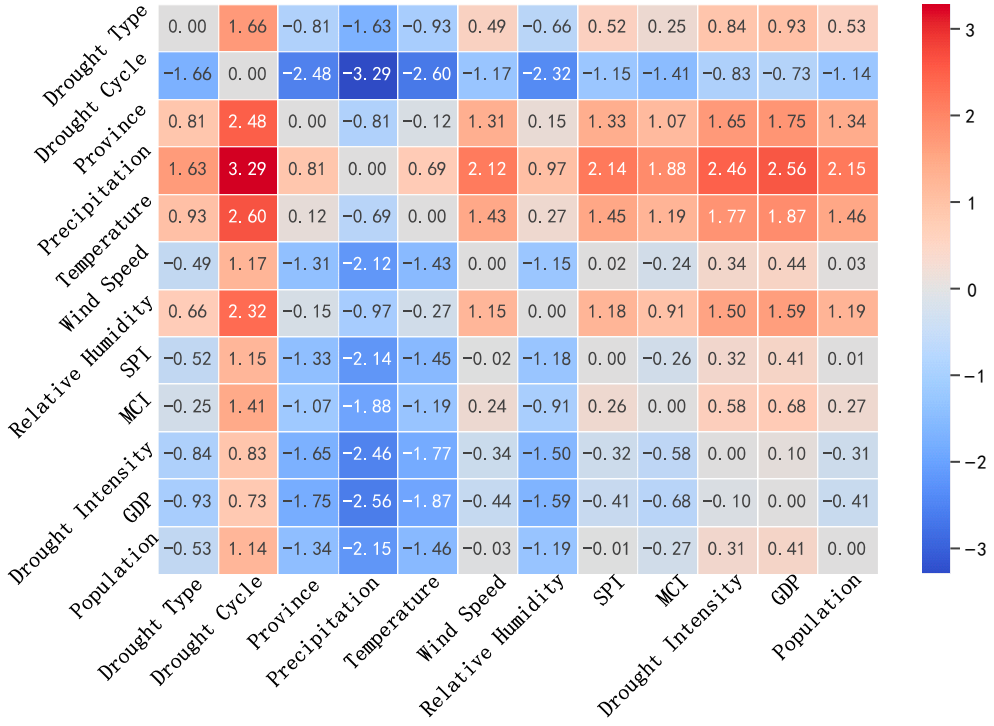


**Figure 8.** Correlation diagram of feature attributes of drought cases.

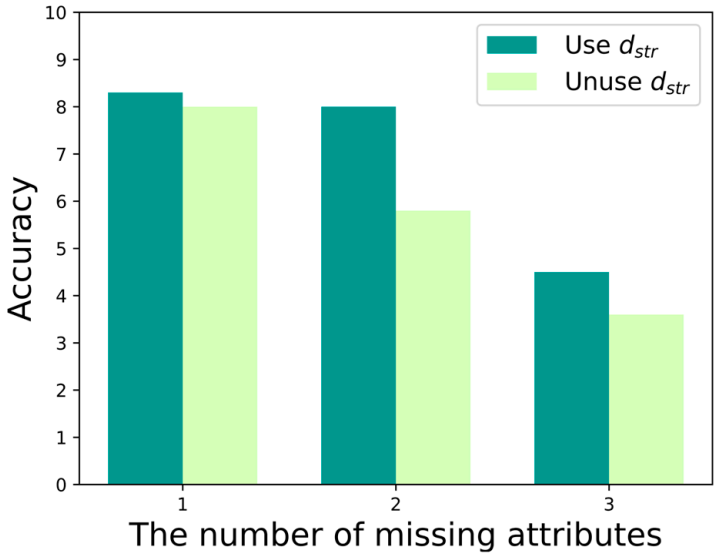


**Figure 9.** Comparison of the average accuracy.

As shown in the figure, the case retrieval algorithm used in this study outperforms other algorithms in terms of accuracy when feature attributes are missing. When two feature attributes are missing, the accuracy of the proposed algorithm is significantly higher than that of the algorithm without the structural coefficient, with an improvement of up to 40%.

Finally, the historical case with the highest similarity to the current case, retrieved by the feature attribute-based case retrieval algorithm, was the 2015 drought case in Yunnan, with a similarity of 75.7%. This result is illustrated in Figure 10.

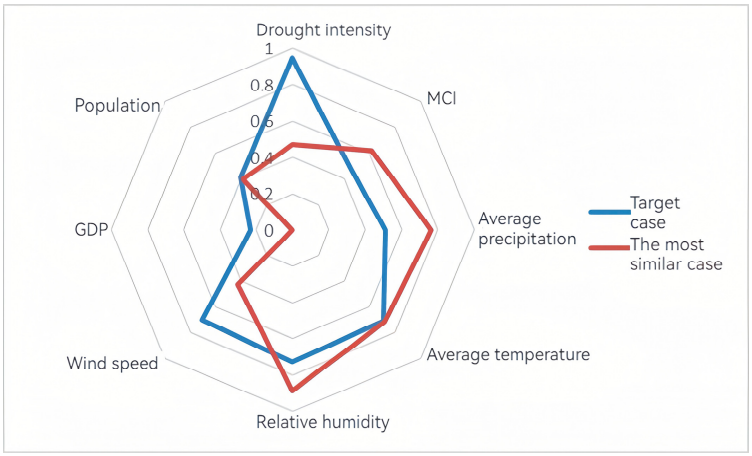


**Figure 10.** Attribute similarity diagram between target cases and historical cases.

2. Case correction results of the DE algorithm

The candidate case generated by the correction algorithm achieves a 94.7% similarity to the target case, surpassing any historical case by 19%. The candidate case suggests a level 4 emergency response with a drought resistance investment of CNY 243 million. Compared with real data from Yunnan Province's spring drought (Table 8), the candidate case's response level aligns with actual requirements. However, its investment is CNY 327 million lower. The fitness function's iteration curve (Figure 11) shows the model's fast and effective convergence.

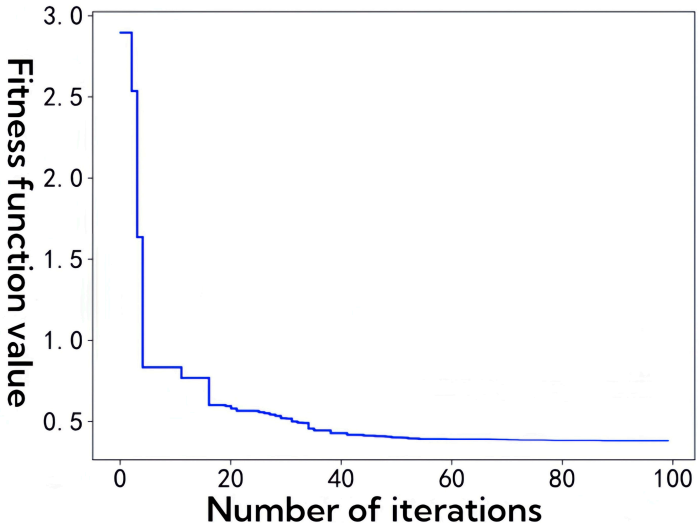


**Figure 11.** Variation in the fitness function.

The research further compares the effectiveness of the proposed algorithm with the particle swarm optimization algorithm, as shown in Figure 12. In Figure 12a, the fitness value of the differential evolution-based case correction algorithm is lower than that of the particle swarm optimization algorithm, indicating faster convergence with fewer iterations. Figure 12b compares the convergence speeds of the two algorithms across multiple iterations. Results indicate that the proposed algorithm converges more rapidly but results in a larger fitness function value upon convergence.

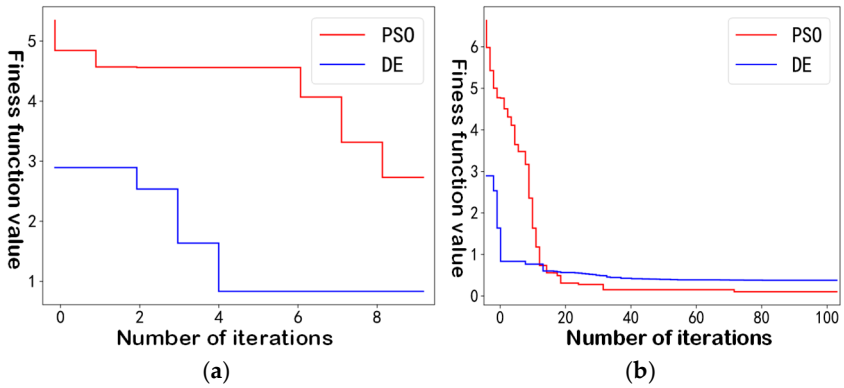


**Figure 12.** Comparative analysis of differential evolution and particle swarm optimization algorithms. (**a**) the results of 10 iterations; (**b**) the results of 100 iterations.

## 3. Results of drought risk assessment in the research area

After revising the emergency response strategy for drought events in Yunnan Province in 2019, the research employs the case correction algorithm based on drought risk assessment to revise the long-term response strategy of the target case. The target case risk assessment results are shown in Figure 13.

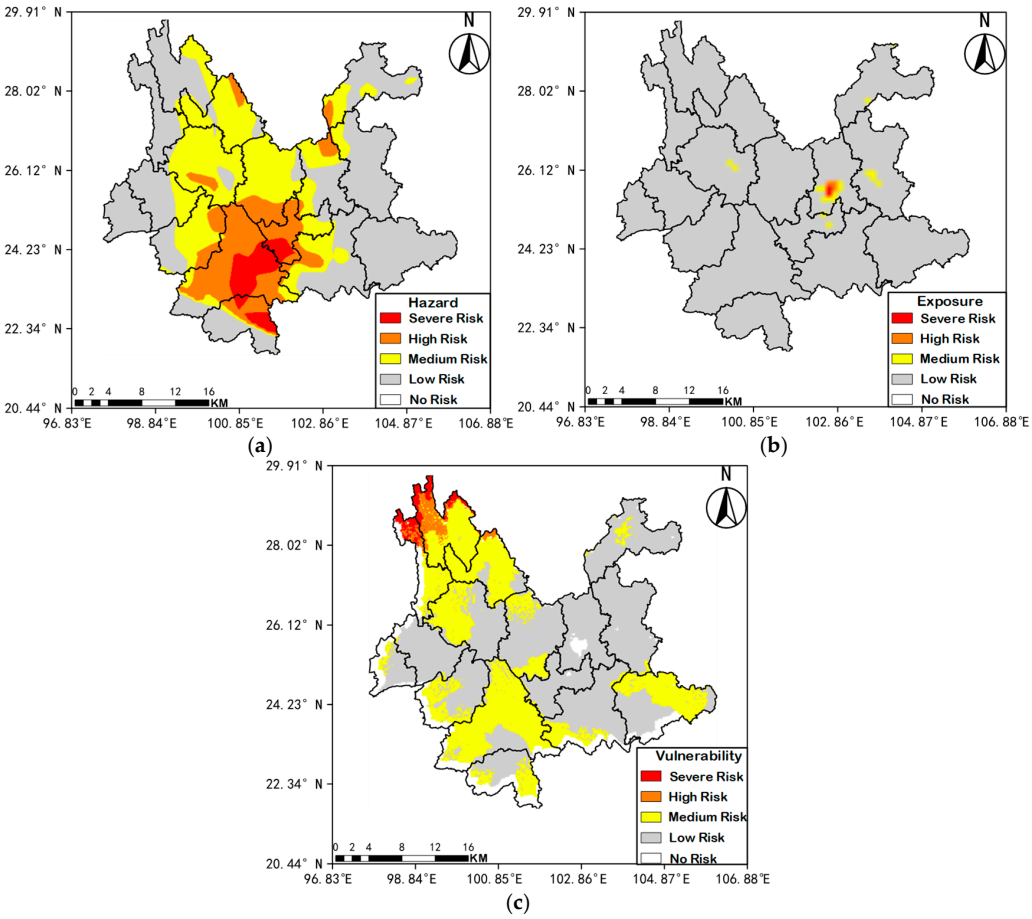


**Figure 13.** Drought risk assessment map of Yunnan Province in 2019. (**a**) The hazard distribution in Yunnan Province; (**b**) the exposure distribution; and (**c**) the vulnerability distribution. In the legend, white represents no risk, gray represents low risk, yellow represents medium risk, orange represents high risk, and red represents very high risk.

The risk assessment map indicates that the highest-risk areas in Yunnan Province were concentrated in the central and southern regions in 2019, among which Pu'er City and Yuxi City had high-risk levels and some areas had extremely high risks. The medium-risk areas were concentrated in the north and west.

Relevant authorities can use the risk maps to reduce risk by adjusting the values of hazard, vulnerability, and exposure indicators. For example, reducing exposure could involve measures to lower population density, while decreasing vulnerability could focus on strategies to alleviate water pressure. By adjusting these indicators, the risk assessment results are impacted, ultimately reducing the overall risk.

4. The modification of long-term response strategies

For the modification of the long-term drought response strategy, the risk level of each region is divided to determine the high-risk area by calculating the hazard, vulnerability, and exposure index of drought, and the corresponding response strategy is recommended according to different risk categories.

The results of the exposure assessment map show that Yunnan Province was generally in a low-risk state in 2019, and the high-risk areas were mainly concentrated in Kunming and its surrounding cities. This is because the value of the exposure index is closely related to the proportion of cultivated land, pastureland, and population density. The proportion of forest land in Yunnan Province is high, while the proportion of cultivated land and pastureland is relatively low. In addition, the population of Yunnan Province is mainly concentrated in big cities such as Kunming, so the drought-affected area is limited. The vulnerability assessment map indicates that the overall vulnerability risk of Yunnan Province in 2019 was moderate. Due to the low GDP and the high proportion of agricultural GDP, the northern region is greatly affected when drought comes, so the vulnerability risk is high. Due to the low dependence on agriculture and the relatively strong water supply capacity, the vulnerability risk of Kunming and other large cities is low.

By assessing the drought risk in Yunnan Province in 2019, this article reveals the distribution features of high-risk regions, high-exposure regions, and high-vulnerability regions of drought. The results showed that the high-risk areas of drought were mainly concentrated in Pu'er City and Yuxi City, the high-exposure area was mainly in Kunming City, and the high-vulnerability area was concentrated in Diqing Tibetan Autonomous Prefecture. According to Formulas (16) and (17), to reduce the exposure risk of Kunming City to medium risk, the change in exposure index is 0.3. The change in population density in Kunming City is 38 people/km$^2$. In other words, if we reduce the population density to reduce the drought exposure of Kunming City, 38 people/km$^2$ should be reduced. The change in exposure risk in Kunming before and after the adoption of quantitative measures is shown in Figure 14.

5. Final result

Combining the results of the two case correction algorithms, the solution of the 2019 drought case in Yunnan Province was finally obtained, as shown in Table 12.

**Table 12.** Table of target case response strategies.

| Category of Measures | Specific Categories | Value |
|---|---|---|
| Emergency measure | Emergency response level | Level 4 |
| | Funding for drought relief | CNY 243 million |

**Table 12.** *Cont.*

| Category of Measures | Specific Categories | Value |
| --- | --- | --- |
| Emergency measure | Given the government's response | 1. Enhance water use efficiency by upgrading irrigation systems and minimizing losses. 2. Encourage drought-resistant crops like wheat and corn to reduce irrigation needs. 3. Enhance water resource management by implementing a drought monitoring system for a secure water supply. |
| | General population response measures | 1.Cultivate drought-resistant plants like succulents and drought-tolerant flowers. 2.Regularly inspect household pipelines for leaks and promptly address any issues. 3. Engage in community, government, and organizational water-saving initiatives to raise awareness about water conservation. |
| Long-term measure | High-risk area | Pu'er City, Yuxi City |
| | High-exposure area | Kunming City |
| | High risk response measures | Optimize water resource distribution, promote rainwater harvesting, adopt water-efficient farming, and advance water-conserving irrigation. |
| | High exposure response measures | We will strictly control the area of cultivated land, implement the policy of returning farmland to forest, strengthen the protection of cultivated land, and reduce the population density by 38 people /km$^2$. |

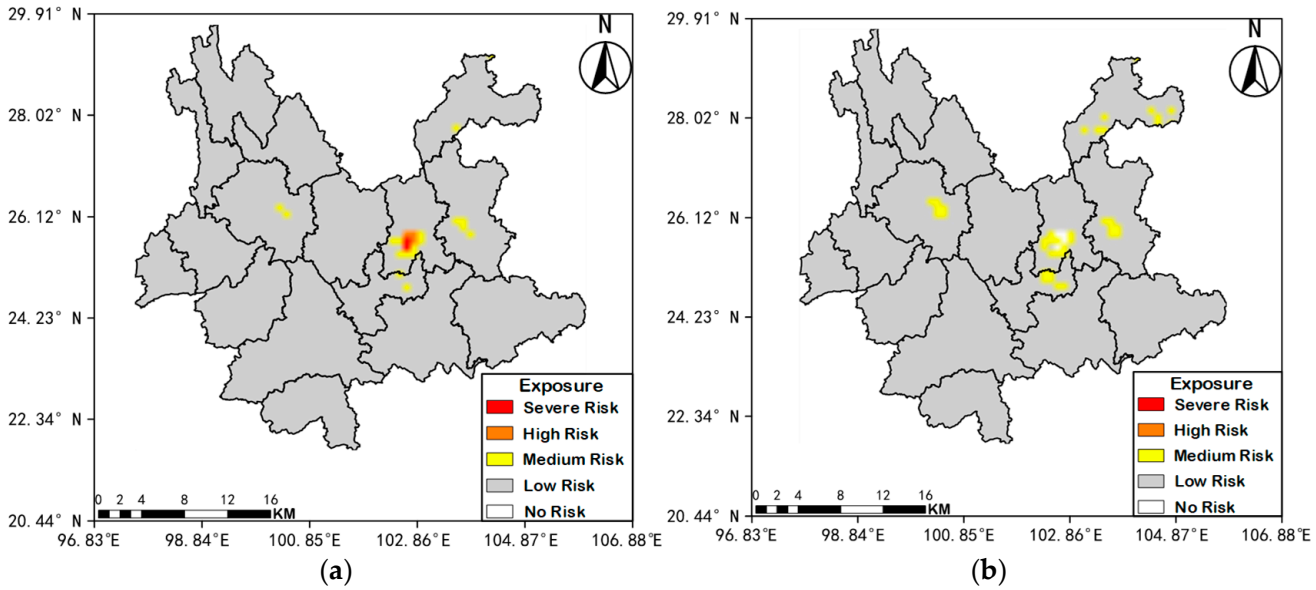


**Figure 14.** Comparison of effects before and after modification of exposure index. (**a**) Before modified index and (**b**) after modified index.

### *3.3. Discussion*

In this research, precipitation, temperature, and other characteristic factors are selected to construct the drought hierarchical structure based on the frame representation method. The run-length theory is used to construct the drought event recognition algorithm to accurately identify the start and end time of drought and drought intensity. The issue

of excessive feature attributes and the varying importance of drought cases in previous studies is addressed by combining the feature attribute similarity case retrieval algorithm with the structural similarity coefficient. For modifying land drought response strategies, a differential optimization algorithm-based emergency strategy modification algorithm was developed, using the target case with high similarity to the initial population. The model generates the candidate case close to the target case through crossover and other operations and then uses the emergency strategy of this case as the solution of the target case. The method solved the problem of the drought event response strategy according to specific cases.

Combining long-term and short-term emergency strategies provides solutions for drought events across different time scales. It addresses the limitations of previous research, which often relied on a single decision-making method and ignored the role of time scales. Furthermore, integrating risk assessment and considering regional characteristics allows for targeted recommendations based on hazard, exposure, and vulnerability in drought-prone areas. This approach resolves the spatial multi-scale analysis issue found in earlier studies.

However, the limitations of this research must be further addressed to meet the requirements of the land drought response.

Although combining the AHP and EWM effectively reduces the subjectivity of result weights, some variables in the model still depend heavily on expert judgment and professional knowledge. This reliance may lead to errors in the results, and future research should address this to enhance objectivity and reliability.

Additionally, the long-term case correction algorithm adjusts measures based on changes in risk assessment results. While it is effective with appropriate feature selection and weights, inaccurate outcomes may occur if the selected indicators are not optimal. Identifying the most reasonable and optimal indicators is an area for future improvement.

This research does not include certain hydrological variables and advanced statistical methods, which are important for drought risk assessment. Reference [35] introduced the Standardized Runoff Index (SRI) and used copula functions for the joint distribution of hydrological drought variables. This highlights the value of incorporating variables like soil moisture, runoff, and groundwater levels into drought research, offering a more comprehensive understanding of drought variation. The use of copula functions can strengthen the analysis and better simulate the non-linear relationships between variables. Their application can improve the understanding of the joint distribution of drought events and lead to more reliable risk assessment results. This method is particularly effective in regions where various environmental factors interact in complex ways.

Finally, the relationship between long-term response measures and regional drought risk values requires further study. Understanding how specific response measures reduce risk values is essential for developing strategies tailored to different drought conditions. Drought impact data and historical response measures can support the quantitative relationship, enabling more targeted and effective measures.

## 4. Conclusions

This research proposes an advanced intelligent recommendation model for drought event response strategies using case-based reasoning (CBR). The model addresses key challenges, such as inaccurate drought case recognition and non-standardized case representations. By selecting key feature factors, including precipitation, temperature, and the Meteorological Drought Index (MCI), a hierarchical drought case structure is constructed using frame representation. A drought recognition algorithm based on run-length theory is used to accurately identify the onset, end, and intensity of drought events. This method achieves over 95% accuracy in drought recognition.

To improve case retrieval, a new algorithm is introduced that combines feature attribute similarity with a case structure similarity coefficient. This approach increases retrieval accuracy by 40% compared to traditional methods that do not consider structural similarity. By integrating both types of similarity, the model advances drought case retrieval, enabling more precise matching and better response strategy recommendations.

A strategy modification algorithm for long-term droughts is also developed. It uses a risk assessment approach that evaluates drought risk, vulnerability, and exposure indices. This algorithm categorizes regions by risk level, allowing for tailored response strategies for high-risk areas. Experimental results show that the risk assessment aligns with real-world conditions, providing valuable support for decision-making in land drought management.

The model can be adapted to other regions by adjusting the key climatic and hydrological factors specific to local conditions, such as precipitation and soil moisture. By recalibrating the algorithms and integrating regional data, the model can provide tailored drought recognition and risk assessment strategies. Future research should focus on enhancing the model's adaptability to different climate zones and exploring the integration of additional hydrological variables, such as groundwater levels and streamflow, to improve risk prediction and mitigation.

**Author Contributions:** Conceptualization, D.T. and Y.Y.; methodology, Y.Y.; software, B.L.; validation, Y.Z.; formal analysis, Y.L. (Yuheng Lei); investigation, Y.L. (Yuheng Lei); resources, B.L.; data curation, Y.L. (Yuxia Li); writing—original draft preparation, Y.L. (Yuheng Lei); writing—review and editing, L.H.; visualization, D.T.; supervision, L.H.; project administration, L.H.; funding acquisition, L.H. All authors have read and agreed to the published version of the manuscript.

**Funding:** This research was funded by the Key Projects of Global Change and Response of the Ministry of Science and Technology of China, grant number 2020YFA0608203; the Science and Technology Support Project of Sichuan Province, grant number 2023YFS0366; and the Fengyun Satellite Application Pilot Program, grant number FY-APP-ZX-2023.02.

**Data Availability Statement:** Data is unavailable due to privacy or ethical restrictions.

**Acknowledgments:** We would like to thank the funding agencies for their financial support, which made this research possible.

**Conflicts of Interest:** The authors declare no conflict of interest.

## References

1. Zaniolo, M.; Fletcher, S.; Mauter, M.S. Multi-Scale Planning Model for Robust Urban Drought Response. *Environ. Res. Lett.* **2023**, *18*, 054014. [CrossRef]
2. Armah, F.A.; Odoi, J.O.; Yengoh, G.T.; Obiri, S.; Yawson, D.O.; Afrifa, E.K. Food security and climate change in drought-sensitive savanna zones of Ghana. *Mitig. Adapt. Strateg. Glob. Chang.* **2011**, *16*, 291–306. [CrossRef]
3. Liu, Z.; Li, W.; Wang, L.; Li, L.; Xu, B. The scenario simulations and several problems of the Sponge City construction in semi-arid loess region, Northwest China. *Landsc. Ecol. Eng.* **2022**, *18*, 95–108. [CrossRef]
4. Li, H.; Gupta, J.; Van Dijk, M.P. China's drought strategies in rural areas along the Lancang River. *Water Policy* **2013**, *15*, 1–18. [CrossRef]
5. Getirana, A.; Libonati, R.; Cataldi, M. Brazil is in Water Crisis—It Needs a Drought Plan. *Nature* **2021**, *600*, 218–220. [CrossRef]
6. Nugraha, A.S.A.; Gunawan, T.; Kamal, M. Modification of Temperature Vegetation Dryness Index (TVDI) Method for Detecting Drought with Multi-Scale Image. *Proc. IOP Conf. Ser. Earth Environ. Sci.* **2022**, *1039*, 012048. [CrossRef]
7. Li, J.; Ren, Y.F.; Dai, Z.J.; Jin, Q.; Shen, C.; Zhang, L. Retrieval of soil moisture at critical period of water demand of winter wheat in Jiangsu Province using MODIS drought index and RBFNN. *Agric. Res. Arid Areas* **2012**, *40*, 251–257.
8. Patel, N.R.; Yadav, K. Monitoring spatio-temporal pattern of drought stress using integrated drought index over Bundelkhand region, India. *Nat. Hazards* **2015**, *77*, 663–677. [CrossRef]

9. Şen, Z. Fuzzy standardized precipitation index (FSPI) for drought early warning procedure. *Theor. Appl. Climatol.* **2024**, *155*, 1281–1287. [CrossRef]
10. Thomaz, F.R.; Miguez, M.G.; de Souza Ribeiro de Sá, J.G.; Alberto, G.W.d.M.; Fontes, J.P.M. Water Scarcity Risk Index: A Tool for Strategic Drought Risk Management. *Water* **2023**, *15*, 255. [CrossRef]
11. Hoover, D.L.; Knapp, A.K.; Smith, M.D. Resistance and resilience of a grassland ecosystem to climate extremes. *Ecology* **2014**, *95*, 2646–2656. [CrossRef]
12. Wang, Y.; Cui, J.; Miao, B.; Li, Z.; Wang, Y.; Jia, C.; Liang, C. Evaluating Performance of Multiple Machine Learning Models for Drought Monitoring: A Case Study of Typical Grassland in Inner Mongolia. *Land* **2024**, *13*, 754. [CrossRef]
13. Zhou, J.; Fan, Y.; Guan, Q.; Feng, G. Research on Drought Monitoring Based on Deep Learning: A Case Study of the Huang-Huai-Hai Region in China. *Land* **2024**, *13*, 615. [CrossRef]
14. Dabanli, I. Drought Risk Assessment by Using Drought Hazard and Vulnerability Indexes. *Nat. Hazards Earth Syst. Sci. Discuss*, 2018; *preprint*. [CrossRef]
15. Stolte, T.R.; de Moel, H.; Koks, E.E.; Wens, M.L.K.; van Veldhoven, F.; Garg, S.; Farhad, N.; Ward, P.J. Global drought risk in cities: Present and future urban hotspots. *Environ. Res. Commun.* **2023**, *5*, 115008. [CrossRef]
16. Gidey, E.; Mhangara, P.; Gebregergs, T.; Zeweld, W.; Gebretsadik, H.; Dikinya, O.; Mussa, S.; Zenebe, A.; Girma, A.; Fisseha, G.; et al. Analysis of drought coping strategies in northern Ethiopian highlands. *SN Appl. Sci.* **2023**, *5*, 195. [CrossRef]
17. Wens, M.; Johnson, J.M.; Zagaria, C.; Veldkamp, T.I. Integrating human behavior dynamics into drought risk assessment—A sociohydrologic, agent-based approach. *Wiley Interdiscip. Rev. Water* **2019**, *6*, e1345. [CrossRef]
18. Tadesse, T. Strategic framework for drought risk management and enhancing resilience in Africa. In Proceedings of the African Drought Conference, Windhoek, Namibia, 15–19 August 2016; pp. 15–19.
19. Melsen, L.A.; Teuling, A.J.; Torfs, P.J.J.F.; Zappa, M.; Mizukami, N.; Mendoza, P.A.; Clark, M.P.; Uijlenhoet, R. Subjective modeling decisions can significantly impact the simulation of flood and drought events. *J. Hydrol.* **2019**, *568*, 1093–1104. [CrossRef]
20. Yan, W.; He, Y.; Cai, Y.; Cui, X.; Qu, X. Analysis of spatiotemporal variability in extreme climate and potential driving factors on the Yunnan Plateau (Southwest China) during 1960–2019. *Atmosphere* **2021**, *12*, 1136. [CrossRef]
21. Fan, X.; Yang, K.; Yang, R.; Zhao, L. Changes in Meteorological Elements and Its Impacts on Yunnan Plateau Lakes. *Appl. Sci.* **2023**, *13*, 2881. [CrossRef]
22. General Administration of Quality Supervision, Inspection and Quarantine of the People's Republic of China; Standardization Administration of China. *GB/T 20481-2017: Grades of Meteorological Drought, 2017*; Chinese National Standard: Beijing, China, 2017. (In Chinese)
23. Xu, Y.; Gao, X.; Shen, Y.; Xu, C.; Shi, Y.; Giorgi, F. A daily temperature dataset over China and its application in validating a RCM simulation. *Adv. Atmos. Sci.* **2009**, *26*, 763–772. [CrossRef]
24. Wu, J.; Gao, X. A gridded daily observation dataset over China region and comparison with the other datasets. *Chin. J. Geophys.* **2013**, *56*, 1102–1111.
25. Wu, J.; Gao, X.; Giorgi, F.; Chen, D. Changes of effective temperature and cold/hot days in late decades over China based on a high resolution gridded observation dataset. *Int. J. Climatol.* **2017**, *37*, 788–800. [CrossRef]
26. Xu, X. China GDP spatial distribution kilometer grid data set. Data Registration and publishing System of Resources and Environmental Sciences Data Center. *Chin. Acad. Sci.* **2017**, *10*, 2017121102.
27. Karavitis, C.A.; Alexandris, S.; Tsesmelis, D.E.; Athanasopoulos, G. Application of the Standardized Precipitation Index (SPI) in Greece. *Water* **2011**, *3*, 787–805. [CrossRef]
28. Cai, X.; Zhang, W.; Fang, X.; Zhang, Q.; Zhang, C.; Chen, D.; Cheng, C.; Fan, W.; Yu, Y. Identification of Regional Drought Processes in North China Using MCI Analysis. *Land* **2021**, *10*, 1390. [CrossRef]
29. Xu, X.; Liu, J.; Zhang, S.; Li, R.; Yan, C.; Wu, S. China multi period land use remote sensing monitoring dataset (CNLUCC). *Resour. Environ. Sci. Data Regist. Publ. Syst.* **2018**.
30. Zhang, M. Deep Sea Emergency Aid Decision Making Based on Case-Based Reasoning Technology Research. Master's Thesis, Dalian Maritime University, Dalian, China, 2020. [CrossRef]
31. Li, K. Research on Comprehensive Pollution Assessment of Heavy Metals in Water Sediments Based on Combination Weighting and Grey Cloud Model. Master's Thesis, Dalian University of Technology, Dalian, China, 2019. [CrossRef]
32. Zhao, J.; Zhang, Q.; Zhu, X.; Shen, Z.; Yu, H. Quantitative assessment of drought risk in China. *Acta Ecol. Sin.* **2021**, *41*, 1021–1031.
33. Carrão, H.; Naumann, G.; Barbosa, P. Mapping global patterns of drought risk: An empirical framework based on sub-national estimates of hazard, exposure and vulnerability. *Glob. Environ. Chang.* **2016**, *39*, 108–124. [CrossRef]

34. Ahmadalipour, A.; Moradkhani, H. Multi-dimensional assessment of drought vulnerability in Africa: 1960–2100. *Sci. Total Environ.* **2018**, *644*, 520–535. [CrossRef]
35. Xiang, Y.; Wang, Y.; Chen, Y.; Bai, Y.; Zhang, L.; Zhang, Q. Hydrological drought risk assessment using a multidimensional copula function approach in arid inland basins, China. *Water* **2020**, *12*, 1888. [CrossRef]